Study of equinoctial asymmetry in the Equatorial Spread F (ESF) irregularities over Indian region using multi-instrument observations in the descending phase of solar cycle 23

S. Sripathi,[1] B. Kakad,[1] and A. Bhattacharyya[1]

[1] In this paper, we present the results of a morphological study of Equatorial Spread F (ESF) irregularities over Indian region based mainly on observations of (1) amplitude scintillations on GPS L-band signal and Rate of TEC Index (ROTI) obtained using a network of GPS receivers and (2) amplitude scintillations on a VHF signal using spaced receivers at Tirunelveli, an equatorial station. Occurrence of both amplitude scintillations on the GPS L1 signal and occurrence of significant ROTI recorded at several stations has been investigated. The latitudinal extent of L-band scintillations shows that their strength is weak over the dip equator but stronger over Equatorial Ionization Anomaly (EIA) region, preferentially during vernal equinox. We find an equinoctial asymmetry in both the occurrence of scintillations and ROTI wherein their occurrence is greater in the vernal equinox than in the autumn equinox. Attempts have been made to understand the asymmetry in latitudinal extent using maximum cross-correlation (C_I) of intensity fluctuations obtained from the VHF spaced receivers observations. The observations suggest that occurrence of C_I less than 0.5 is more in the vernal equinox than in the autumn equinox suggesting that the maximum height of the Equatorial Plasma Bubbles (EPBs) during vernal equinox may be higher than that during autumn equinox. TIMED/GUVI retrieved peak electron density during the same period also indicates that background electron density is higher and more symmetric during vernal equinox than autumn equinox. Hence, our results suggest that background electron density may be playing a vital role in creating the equinoctial asymmetry.

1. Introduction

[2] The irregularities in the nighttime equatorial ionosphere have been studied for several decades using ground-based coherent radars, ionospheric scintillation observations, optical airglow, in situ rocket, and satellite based observations to understand their occurrence pattern and varying characteristics from one night to another [e.g., *Fejer and Kelley*, 1980; *Kelley*, 2009]. Irregularities of the nighttime equatorial ionosphere called Equatorial Spread F (ESF) irregularities are found to vary with season, latitude, longitude, solar, and magnetic activity [e.g., *Chandra and Rastogi*, 1972; *Sastri et al.*, 1979; *Fejer and Kelley*, 1980; *Aarons*, 1993; *Huang et al.*, 2002; *Burke et al.*, 2004; *Lee et al.*, 2005; *Manju et al.*, 2007]. The ESF irregularities span a large range of scale sizes extending over several orders of magnitude. Of these the intermediate scale length (~100 m to a few km) irregularities cause scintillation on VHF, UHF, and L-band signals. The

intermediate scale length irregularities are generated by the Rayleigh-Taylor (R-T) instability on the bottomside of the post-sunset equatorial F region which may cause a plasma depleted region referred to as the equatorial plasma bubble (EPB) to rise to the topside and develop smaller scale structures. Low cost systems like scintillations observed on UHF/VHF signal transmitted from a geostationary satellite and recorded using single and spaced ground receiver systems have been extensively used to monitor the intermediate scale length irregularities [e.g., *Basu and Kelley*, 1977; *Basu et al.*, 1978; *Yeh and Liu*, 1982; *Aarons*, 1993; *Bhattacharyya et al.*, 1992, 2001; *Ray and Dasgupta*, 2007]. In recent times, due to the advent of GPS observations, GPS derived Total Electron Content (TEC) and amplitude scintillations on L1 signal have also been extensively used for such studies [e.g., *Kelley et al.*, 1996; *Pi et al.*, 1997; *Musman et al.*, 1997; *Bhattacharyya et al.*, 2000; *Valladares et al.*, 2004; *Rama Rao et al.*, 2006a, 2006b; *Sripathi et al.*, 2008; *Muella et al.*, 2008]. These irregularities are highly field aligned and therefore, when they reach higher altitude, its latitudinal extent may reach the Equatorial Ionization Anomaly (EIA) region to produce strong irregularities across the spectrum of intermediate scale sizes because the background electron density

[1]Indian Institute of Geomagnetism, Navi Mumbai, India.

is relatively higher as compared to that of the dip equator. Hence, scintillations observed on UHF/VHF signals transmitted from a geostationary satellite recorded at equator and EIA region have been extensively used to monitor the relative strengths of intermediate scale length irregularities at equator and crest region [e.g., *Bhattacharyya et al.*, 2003].

[3] Several morphological studies on ESF irregularities have been made earlier over Indian region in the high solar activity period using ionosondes, radars, and scintillation studies [e.g., *Chandra and Rastogi*, 1972; *Krishna Moorthy et al.*, 1979; *Rastogi*, 1980; *Rastogi et al.*, 1990; *Devasia et al.*, 2002; *Jyoti et al.*, 2004; *Patra et al.*, 2005; *Rama Rao et al.*, 2006c], while few attempts have been made during low solar activity period due to lack of observations [e.g., *Rastogi et al.*, 1990; *Rama Rao et al.*, 2006a, 2006b, 2006c]. The morphological studies over Indian region indicate the following characteristics: (1) the ESF irregularities occur mostly following the post sunset rise of F layer; (2) scintillations associated with range spread F shows fast fading rates, while scintillations associated with frequency type spread F shows slower fade rates; (3) occurrence of scintillations decreases with increase in frequency and earlier onset of scintillations on lower frequencies than on higher frequencies; (4) occurrence of scintillations during (post-) pre-midnight period is high during (low) high sunspot activity period; (5) scintillations occur mainly in the pre-midnight period during equinoxes but mostly scintillations are seen in the post-midnight period during summer months; (6) occurrence of scintillations are correlated with solar flux; (7) while equatorial scintillations are found to occur as a single patchy, discrete patches are found to occur at low latitudes; and (8) weak L-band scintillations occur over equator but strong scintillations occur over EIA region.

[4] While many studies have been made to understand/ characterize the different plasma processes involved in the generation of these irregularities, only few studies have explored the causes for the seasonal and longitudinal variability in their occurrence [*Maruyama and Matuura*, 1984; *Tsunoda*, 1985; *Abdu et al.*, 1981; *Burke et al.*, 2004]. *Maruyama and Mathuura* [1984] using satellite observations suggested that while the background electron density distribution tends to be symmetric about the magnetic equator in the regions of enhanced ESF activity, it tends to be asymmetric about the magnetic equator when the ESF activity is a minimum. Based on these observations they suggested that transequatorial neutral winds might suppress the ESF irregularities. On the other hand, *Tsunoda* [1985] and *Abdu et al.* [1981] have found enhanced ESF activity when local sunset takes place simultaneously at the conjugate E regions in which case the eastward polarization electric field is slightly enhanced and provides maximum vertical drift that is required for ESF generation. This indicates existence of an important relationship between solar terminator and magnetic field declination for the ESF irregularities to develop. These two observations suggest that plasma bubbles are likely to develop under the following conditions: (1) sunset terminator is approximately aligned with the geomagnetic flux tube connecting the equatorial F region to conjugate E regions and (2) negligible thermospheric winds along the geomagnetic meridian. This happens only during equinoctial periods over Indian region [e.g., *Chandra and Rastogi*, 1972; *Rama Rao et al.*, 2006c]. Under these conditions, a seed perturbation

such as gravity waves can trigger the Rayleigh-Taylor (R-T) instability [e.g., *Sultan*, 1996]. While these hypotheses seem to explain some of the observations in terms of seasonal and longitudinal variability, still uncertainties exist in understanding and predicting these irregularities [e.g., *Abdu*, 2001]. This is partly due to the fact that since the ESF irregularities are observed using radio waves in different frequency bands, ESF irregularity pattern appears to be different in different frequency bands as the evolution of plasma irregularities of different scale sizes present in the ESF spectra also depend on the ambient conditions.

[5] In this paper, we present a study on the equinoctial asymmetry in the occurrence of scintillations on L-band and VHF band signal and occurrence of significant variation in the TEC as measured by the Rate Of TEC Index (ROTI) and also their latitudinal extent over Indian region. Earlier studies indicated that equinoctial asymmetry in the occurrence of L-band scintillations may be attributed to differences in the meridional winds during two equinoxes [e.g., *Nishioka et al.*, 2008; *Maruyama et al.*, 2009; *Otsuka et al.*, 2006]. However, the earlier studies on equinoctial asymmetry were based only on few station observations. Here, we study equinoctial asymmetry in the latitudinal variation of both occurrence of L-band scintillations and occurrence of ROTI using several stations right from the equator to the equatorial ionization anomaly (EIA) over Indian longitude region, which has not been presented earlier. Hence, in this paper, we present a morphological study of L-band scintillations produced by irregularities with scale size of ~400 m over Indian region using GAGAN (GPS Aided Geo-Augmented Navigation) network during the years 2004–2005, which is on the descending phase of solar activity period, and compare them with VHF spaced receivers scintillations produced by irregularities of scale size of ~1 km observations, and along with peak electron density of the F2 region obtained from TIMED GUVI. It may be mentioned that while some studies have been made earlier over Indian region using GAGAN network in the descending phase of solar cycle 23 [e.g., *Rama Rao et al.*, 2006a, 2006b, 2006c; *Sripathi et al.*, 2008], we here present morphology of the scintillations that show some new observations such as equinoctial asymmetry in the occurrence of scintillations on the VHF-band signals as well as equinoctial asymmetry in the latitudinal variation of occurrence of scintillations on the L-band and ROTI over Indian region.

2. Experimental Details

[6] The GPS data presented here are obtained under GAGAN project using a network of dual frequency GPS receivers to study the equatorial and low latitude ionosphere over Indian region and also to model the ionosphere in this region for use in aviation [*Rama Rao et al.*, 2006a]. Figures 1a–1b show the location of GPS receiver stations and their geomagnetic field line connection to the equatorial F region, respectively. Table 1 gives the geographic and geomagnetic latitudes and longitudes of GPS receiver stations. The kind of receiver that is being used to collect the TEC and scintillations data is GSV 4004 Ionospheric Scintillation Monitor (ISM) [*Van Dierendonck et al.*, 1996; *Rama Rao et al.*, 2006b]. The GPS satellites basically transmit radio signals at two frequencies namely L1 (1575.42 MHz) and L2 (1227.60 MHz) [*Mannucci et al.*, 1999]. Due to the dispersive
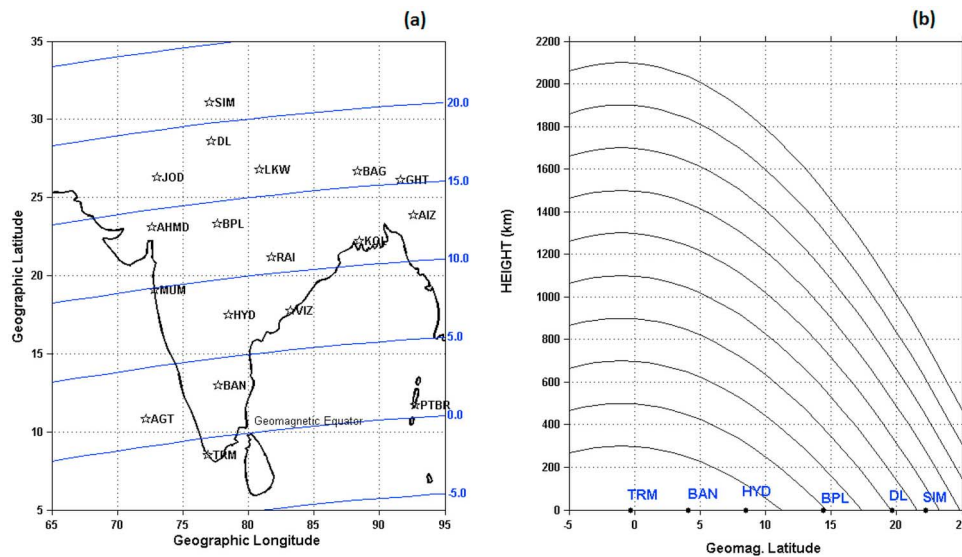
Figure 1. (a–b) A location of GPS receiver stations and sketch of their field line connecting to the equatorial ionosphere.

nature of the ionosphere, these two radio signals propagate at different velocities and produce a time delay for each signal by a certain amount that is generally much smaller than the total transit time and is proportional to the total electron content along the line of sight to the satellite. Using this time delay along with the more accurate phase information, the slant TEC (STEC) is obtained. It may be noted that each GPS receiver can track up to 11 GPS C/A-code signals at L1 frequency (1575.42 MHz). The data collected at every 1 min interval are used to obtain the statistical parameters like S_4 index, which is the standard deviation of normalized intensity of the signal, standard deviation of phase, receiver lock time, etc., for each satellite being tracked. Scintillations are produced when the radio signals travel through a turbulent medium, where changes in the refractive index produce scattering. If the irregularities are confined to a layer of thickness of less than 100 km, when the radio waves emerge from the irregularity layer only a significant phase perturbation is imposed due to the irregularities. Further propagation of the radio waves to the plane of the receiver produces amplitude fluctuations in addition to phase fluctuations. For weak scintillation, maximum contribution to the amplitude fluctuation comes from irregularities having scale size of the first Fresnel zone. For GPS, this scale works out to be ~400 m. Hence, GPS L-band scintillations require the presence of a few hundred meters scale size irregularities. The 'S$_4$ Index' is used to monitor the strength of amplitude scintillations on L1 frequency. The S_4 index and STEC data thus recorded are processed for each of the satellite passes with an elevation mask angle greater than 30° so as to minimize the effects of multipath and tropospheric scattering.

[7] VHF spaced receiver scintillation observations obtained at Tirunelveli, an equatorial station, are used in conjunction with data from a network of GPS receivers data during the same period to understand the irregularity characteristics. The geostationary satellite UFO2 located at 71.2°E transmits a signal at 251 MHz and is received by ground VHF receivers separated by a distance of 540 m in the magnetic east-west direction [e.g., *Bhattacharyya et al.*, 2001]. For weak scin-

tillations, maximum contribution to the amplitude fluctuation comes from irregularities having scale size of the first Fresnel zone, which is ~1 km for a 251 MHz signal. This spaced receiver system can provide details about the nature of the irregularities such as maximum cross-correlation between intensity variation (C_I) recorded by the two receivers, turbulence parameter (V_c), and mean zonal drift velocity (V_0) as a function of local time computed using full cross-correlation analysis [*Briggs*, 1984] in addition to S_4 index. Using the maximum cross-correlation (C_I), we can determine whether the irregularities over head are freshly generated or drifted in from west.

[8] TIMED-GUVI (Global Ultra Violet Imager) satellite limb data for the years 2004–2005 is analyzed to obtain the F2 layer peak electron density on a global scale during local nighttime [e.g., *DeMajistre et al.*, 2004]. TIMED GUVI is in

Table 1. List of GPS Receiver Locations Installed in India Under GAGAN Project

Station Number	Station Name	Geo. Lat. (°N)	Geo. Long. (°E)	Geom. Lat. (°N)	Geom. Long. (°E)
1	Jodhpur (JOD)	26.26	73.05	17.75	147.16
2	Delhi (DL)	28.58	77.21	19.68	151.29
3	Bangalore (BAN)	12.95	77.68	4.08	150.24
4	Hyderabad (HYD)	17.45	78.47	8.49	151.41
5	Bhopal (BPL)	23.29	77.62	14.38	151.14
6	Lucknow (LKW)	26.76	80.88	17.57	154.53
7	Simla (SIM)	31.08	77.066	22.18	151.42
8	Agatti (AGT)	10.83	72.17	2.49	144.65
9	Trivandrum (TRM)	8.48	76.92	−0.31	149.08
10	Bagdodra (BAG)	26.68	88.32	16.99	161.46
11	Aizwal (AIZ)	23.84	92.62	13.94	165.32
12	Guwahati (GHT)	26.12	91.59	16.26	164.48
13	Kolkatta (KOL)	22.18	88.44	12.49	161.28
14	Raipur (RAI)	21.18	81.74	11.94	154.86
15	Vizog (VIZ)	17.75	83.22	8.41	155.99
16	Mumbai (MUM)	19.09	72.85	10.64	146.18
17	Ahmedabad (AHMD)	23.064	72.62	14.61	146.40
18	Portblair (PTBR)	11.67	92.725	1.78	164.83
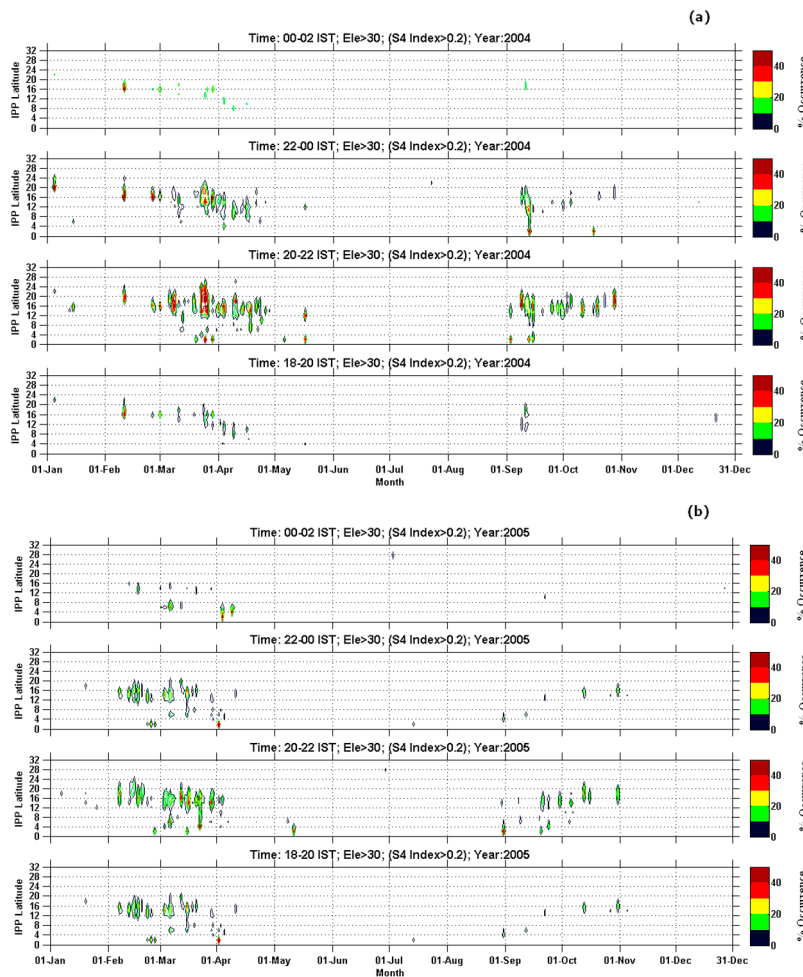
Figure 2. The seasonal and latitudinal variation of L-band scintillations at 18:00–20:00 IST, 20:00–22:00 IST, 22:00–00:00 IST and 00:00–02:00 IST during the years (a) 2004 and (b) 2005, respectively. Here the elevation of 30°, longitude of 75°–80° and S4 > 0.2 are used as thresholds.

a near circular orbit at 625 km altitude with inclination of about 74°. GUVI is a far ultraviolet (115–180 nm) scanning spectrograph imager that measures optical emissions in the 135.6 nm band. The emissions in this band are proportional to square of the electron density; hence, through tomographic inversions the electron density profiles and the F2 layer peak, electron densities can be retrieved.

3. Observations

3.1. General Characteristics

[9] In this section, we present the general morphology of the L-band scintillations such as seasonal and latitudinal variations over Indian region. Figures 2a–2b show the seasonal and latitudinal variation of percentage of occurrence of L-band scintillations as a function of day number at every 2 h interval for the years 2004 and 2005, respectively. These figures are obtained after combining 18 stations data with longitudes restricted to 75–85°E, elevation angle >30° and S_4 index >0.2. Observations presented here suggest that the occurrence of weak to moderate scintillations has been much more frequent during the year 2004 than during the year 2005, when the scintillations have been generally weaker than in

2004. Also the observations reveal that there is greater occurrence of L-band scintillations beyond 00:00 IST during vernal equinox period than in autumn equinox period. Further, observations suggest that while L-band scintillations mostly occur during the months of March and April in 2004, L-band scintillations mostly occur in the months of February and March during 2005. Keen observations reveal that the latitudinal extent of L-band scintillations exhibits seasonal variation where they slowly descend/ascend to higher latitudes as day number progresses, indicating that height of the ESF irregularities varies with season. However, there is not much difference seen in terms of longitudinal variation over Indian longitude belt (not shown here). Except on few occasions, we have not seen any L-band scintillations during geomagnetic storms.

[10] The rate of TEC Index (ROTI) which is a proxy for the density fluctuations in the ionosphere is studied next. It is obtained using the technique discussed by *Pi et al.* [1997], which can be mathematically written as $\sqrt{\langle ROT^2 \rangle - \langle ROT \rangle^2}$ where ROT is rate of change in TEC in TEC units/min (1 TECU = 1×10^{16} electrons/m^2). ROTI is defined as the standard deviation of ROT over a 5 min interval [e.g.,
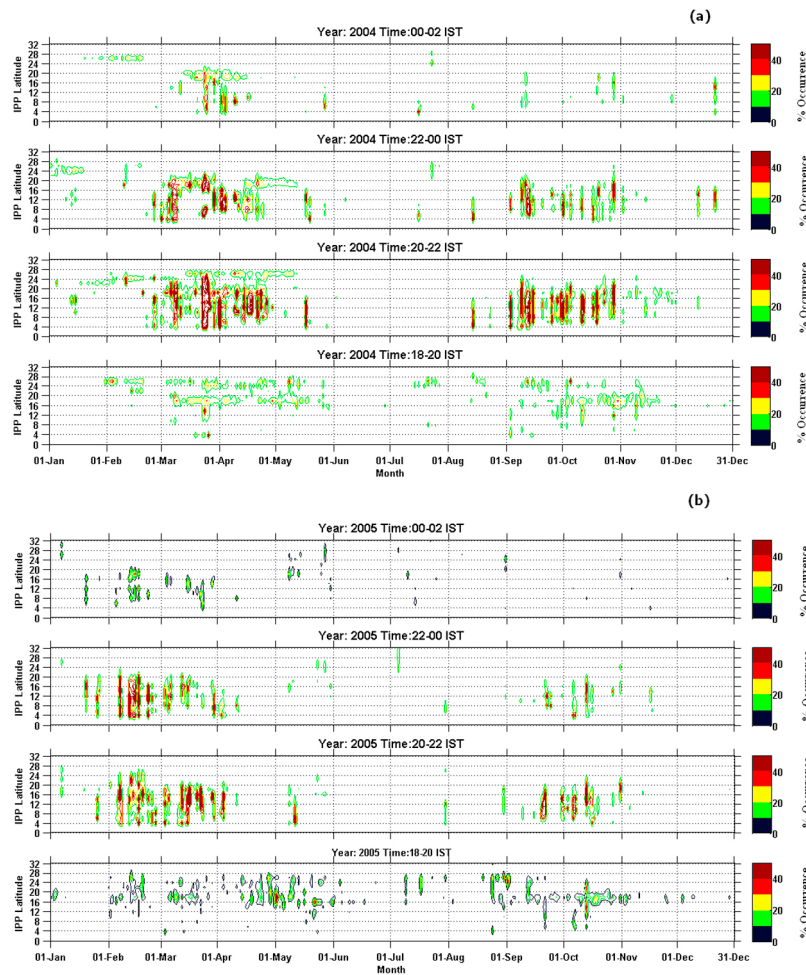
Figure 3. The percentage of occurrence of seasonal and latitudinal variation of ROTI at 18:00–20:00 IST, 20:00–22:00 IST, 22:00–00:00 IST and 00:00–02:00 IST during the years (a) 2004 and (b) 2005, respectively. Here the elevation of 300, longitude of 75–850 and ROTI > 0.3 are used as thresholds.

Pi et al., 1997; *Bhattacharyya et al.*, 2000; *Nishioka et al.*, 2008]. The ROTI has been used as a parameter to identify the small scale density fluctuations to study ionospheric irregularities and TIDs. It may be noted that the shortest irregularity scale size that ROT and hence contribute to ROTI is ~6 km scale size irregularities when assuming the drift velocity of the ionospheric plasma irregularities to be about 100 m/s. However, L-band scintillations are caused due to scale sizes of ~400 m. The range of ROTI values usually lies between 0 and 5 TEC units/min. By choosing a threshold value of ROTI, one can identify km scale density fluctuations [e.g., *Pi et al.*, 1997; *Nishioka et al.*, 2008]. Here while calculating the occurrence percentage of ROTI over a given IPP latitude for a given time interval, we kept a threshold value of ROTI >0.3 TECU/min and restricted our study to longitudes between 75 and 85°E. Figures 3a–3b show the seasonal and latitudinal variation of percentage of occurrence of ROTI as a function of day number at every 2 h interval for the year 2004 and 2005 respectively. These figures are obtained in a similar fashion as Figures 2a–2b. Observations presented here suggest that the occurrence of ROTI >0.3 TECU/min has been much more frequent during the year 2004 than during the year 2005. Also the observations reveal that the occurrence of

ROTI >0.3 TECU/min have been found beyond 00:00 IST much more frequently during vernal equinox period than during autumn equinox period. Further, it is seen from these figures that while occurrence of ROTI is mostly seen during March and April in 2004, ROTI tend to occur in February and March but not in April during 2005 which is similar to L-band scintillation occurrence plotted in Figures 2a–2b. There is some occurrence of ROTI >0.3 TECU/min in the months of May–June that are not revealed in the L-band scintillations, which could be due to differences in the scale size of the irregularities detected by these two parameters.

3.2. Comparison of L-band Scintillations During Vernal and Autumn Equinox Period

[11] In order to study the distribution of L-band scintillations according to strength as measured by the S_4 index at different latitudes, we have plotted the histogram plots for vernal and autumn equinox periods separately after combining the years 2004 and 2005 in Figures 4a–4b. From the figure, it can be seen that the distribution of S_4 index over equatorial latitudes during both equinoxes are found to be equal, while there exists clear-cut difference in the strength of S_4 index over higher latitudes, where we noticed S_4 index
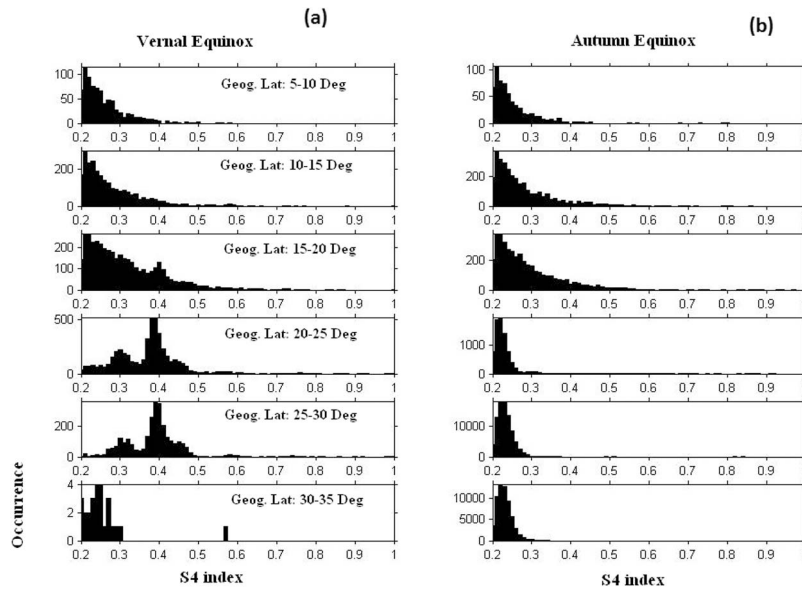
Figure 4. The histogram plots during (a) vernal equinox and (b) autumn equinox periods at every 5° latitude after combing 2004 and 2005 data.

of 0.4 or more is dominant during vernal equinox while they are absent for autumn equinox period.

3.3. Comparison With Peak Electron Density of F2 Layer Over Equatorial Region

[12] Figures 5a–5b show the latitudinal variation of mean peak electron density (N_mF_2) obtained from TIMED GUVI satellite over Indian longitude region during 19:30–20:30 IST during vernal and autumn equinox periods during the years 2004 and 2005 respectively. It may be noted that GUVI satellite traverses through all local times every 60 days. From the figure, it is evident that latitudinal distribution of N_mF_2 during vernal equinox is more symmetric about magnetic equator than during autumn equinox for both 2004 and 2005
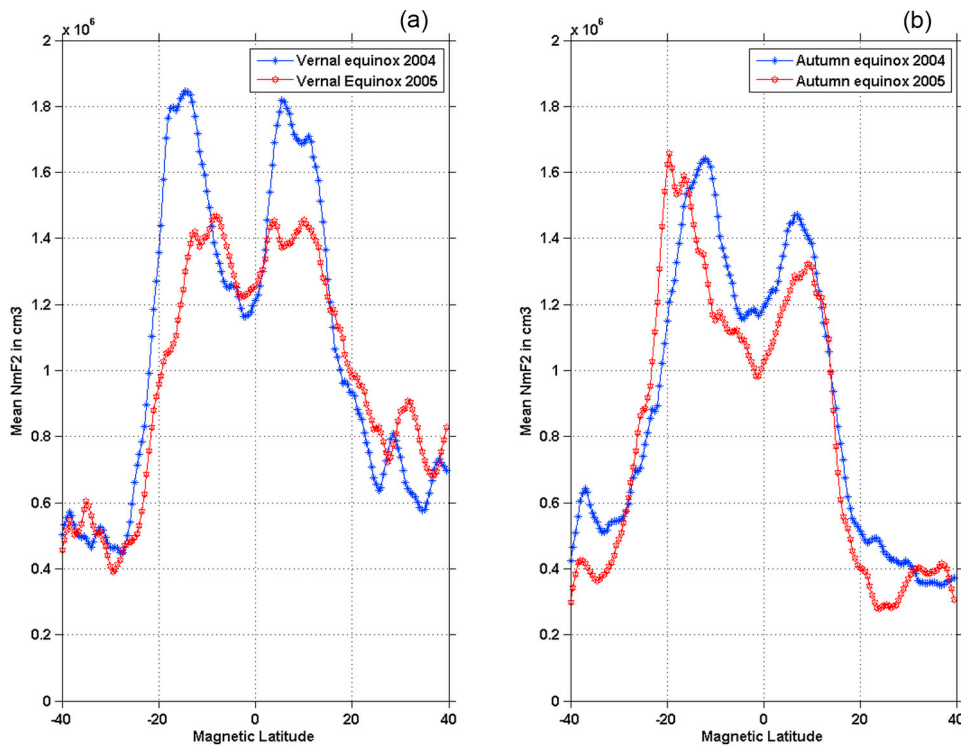
Figure 5. The latitudinal variation of mean NmF2 during (a) vernal and (b) autumn equinox periods at 19:30–20:30 IST during the years 2004 (asterisk) and 2005 (hexagon) over Indian longitude as obtained from the TIMED GUVI satellite.
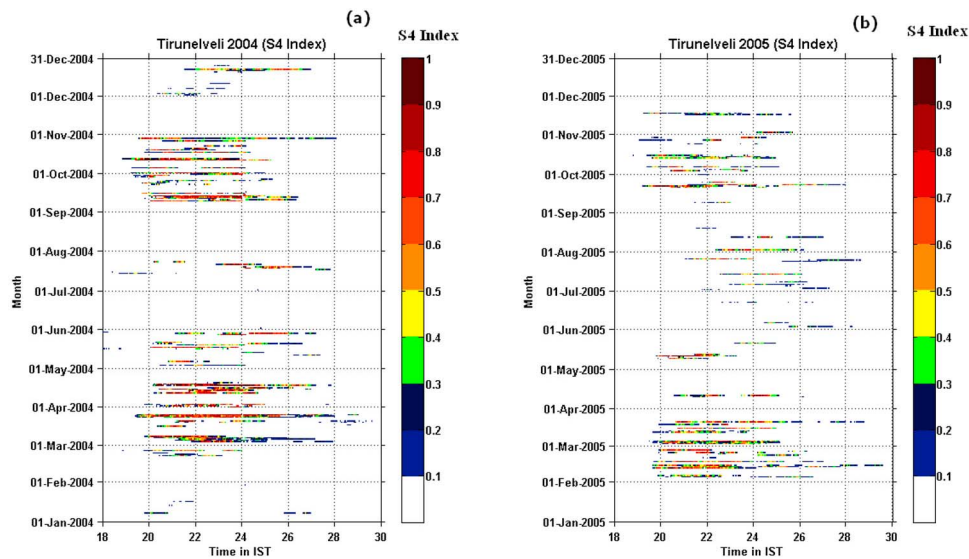
Figure 6. The S_4 index on the VHF signal over Tirunelveli, an equatorial station for the years (a) 2004 and (b) 2005, respectively.

and the crest regions are expanded to higher latitudes during vernal equinox suggesting that zonal electric field could also be higher during vernal equinox as compared to autumn equinox for the year 2004. The figure also suggests that vernal equinoctial months have higher N_mF_2 compared to autumn equinoctial months. For 2005, the large asymmetry around magnetic equator may be responsible for suppression of scintillations during autumn equinox. A possible source of higher N_mF_2 in the southern latitudes during autumn equinox may be the enhanced lower atmosphere convective activity in this period [e.g., *Kumar et al.*, 2007]. The observations also indicate that peak N_mF_2 decreases from 2004–2005 as solar flux decreases. It should be mentioned here that while mean F10.7 cm solar flux values are 106.8 and 104.5 during vernal and autumn equinox respectively for the year 2004, it has values of 88.0 and 83.6 respectively during vernal and autumn equinox period for the year 2005. So, the difference between the vernal and the autumn equinox is not as significant as annual variation.

3.4. Comparison With VHF Scintillations

[13] In order to understand and compare the L-band scintillations with VHF scintillations, we have plotted the VHF scintillation index at every 3 min interval observed over Tirunelveli, an equatorial station during 2004–2005 in Figures 6a–6b. Here, while x axis represents time in IST, y axis represents the Julian day number. The data is collected on all nights. The white space in the figure indicates that S_4 index is less than 0.1. The observations suggest that stronger VHF scintillations are observed during vernal equinox period during both 2004 and 2005 as compared to that of autumn equinox period. The observations also suggest that VHF scintillations during vernal equinox period are present for longer duration than that during autumn equinox period. While there is no noticeable time difference noticed in the initial occurrence of scintillations between autumn and vernal equinox periods, where most of the scintillations are found to start around 19:00–19:30 IST, scintillations in the June solstice have been reported to occur later at night at about

22:00 IST and most of these scintillations are prolonged in the post-midnight until 03:00 IST. It is interesting to note that the MST radar observations obtained in the June solstice in the ionospheric mode at Gadanki, India also reveal that ~3 m scale size irregularities have been noticed frequently during post midnight period, which were found to be significantly different from the normal post sunset ESF irregularities reported [*Patra et al.*, 2009].

4. Discussion

[14] The observations presented in section 3 suggest the following: (1) weak L-band scintillations over equatorial region during both equinoxes and (2) strong L-band scintillations in and around the crest region occur during vernal equinox. The latitudinal and temporal variation of L-band scintillations is found to be quite similar to that of latitudinal and temporal variation of occurrence characteristics of ROTI. In addition, the observations also suggest that while L-band scintillations are more dominant for both equinoctial months as compared to the solstice months, there exists some significant difference between the two equinoxes. The observations suggest that there exists an asymmetry in the occurrence of scintillations as well as the latitudinal extent of scintillations for these two equinoctial periods during the years 2004 and 2005. Observations suggest that occurrence of L band scintillations is greater in the vernal equinox than in the autumnal equinox, and the occurrence of scintillations is found to extend to the higher latitudes during the vernal equinox than for the autumn equinox. The observations indicate that the scintillations are also found to be stronger in 2004 than in 2005. These observations are in accordance with latitudinal variation of occurrence of ROTI. Scintillations on a VHF signal recorded during the same period at an equatorial station also indicate that (1) strength of S_4 index and (2) duration of scintillations is longer in the vernal equinox than during the autumn equinox. Simultaneous observation of mean peak electron density (N_mF_2) from TIMED GUVI satellite in the nighttime reveals some significant
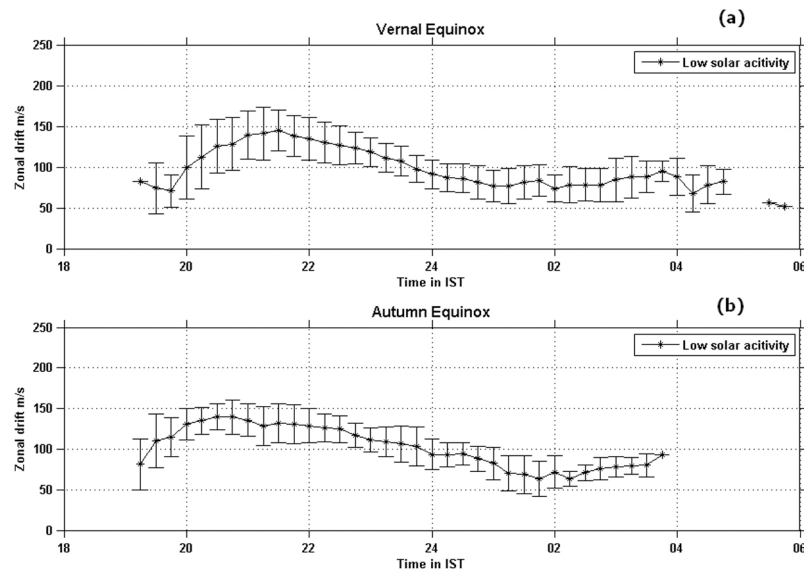
Figure 7. The temporal variation of zonal drift velocity during (a) vernal and (b) autumn equinox period during 2004–2005.

enhancements in the background electron density during vernal equinox than that of autumn equinox in both the years 2004 and 2005, although for the same season nighttime N_mF_2 on the Indian longitude region is higher in 2004 than in 2005. It may be noted that we have also looked into solar flux differences between the vernal and autumn equinox periods as the differences in the occurrence of scintillations during these two equinoxes could be associated with differences between the solar flux values. We have noticed that the difference between the vernal and the autumn equinox is not significant.

[15] *Dasgupta et al.* [1983] have studied the F region ionization differences between vernal and autumn equinox over equatorial and low latitude regions at different longitudes during the year 1979 and found that vernal equinox has enhanced TEC than autumn equinoxes. They suggested that causes for the asymmetry seen in their observations could be due to changes in the neutral composition during these two equinoxes. *Ray and Dasgupta* [2007] have studied the scintillation characteristics at L-band near the crest of equatorial ionization anomaly over Kolkata (22.58°N, 88.38°E, geomagnetic Lat: 13.04°N) using geostationary satellite INMARSAT (64°E) during 1996–2000 and found that there exists an asymmetry in the occurrence of scintillations between the equinoxes. They have attributed this to the difference in ambient ionization between the two equinoxes resulting from composition changes. Recently some observations have been reported from Kototabung, Indonesia by *Otsuka et al.* [2006] using spaced GPS receivers operated in single frequency mode. They have reported that occurrence rate of L-band scintillations is higher during March–April than in September–October during low solar activity period. Using few cases of zonal drift velocity obtained using spaced GPS receivers data during these two equinoxes, they have suggested that east-west component of plasma drift velocity may be related to the evolution of plasma irregularities causing Pre-Reversal Enhancement (PRE) of eastward electric field and therefore leading to the enhanced scintillations

during March–April months, while cause for the asymmetric zonal drift velocity as seen by them during these two periods are attributed to the asymmetric meridional winds in the thermosphere. In order to examine the asymmetric zonal drifts over Indian longitude, we have also looked into the zonal drift velocity obtained from the spaced VHF receiver's scintillations over Tirunelveli during both vernal and autumn equinox periods respectively. Figures 7a–7b show the mean zonal drift velocity during vernal and autumn equinox period during 2004–2005. The observations show that not much difference in zonal drift velocities is noticed between vernal and autumn equinox periods. Using MU radar observations, *Balan et al.* [1997] have studied the asymmetry in the electron density along with temperature and plasma drift velocity data. They have noticed that while electron density at the bottomside of ionospheric F region is somewhat greater in autumn equinox period compared to vernal equinox, at higher altitudes the asymmetry reverses and becomes very strong, with electron density during vernal equinox exceeding 150% of that of autumn equinox. They have attributed this asymmetric distribution of electron density to asymmetry in the neutral winds. *Nishioka et al.* [2008] have shown the occurrence characteristics of plasma bubbles using GPS TEC obtained all over the globe and found equinoctial asymmetry in the occurrence of plasma bubbles in the Asian region. They have suggested that equinoctial asymmetry could be due to asymmetric distribution of integrated conductivities during these equinoctial periods. Recently, *Maruyama et al.* [2009] have studied the equinoctial asymmetry in detail using three ionosondes, where one is located at equator and other two were located on either side of the equator, along with SAMI3 model results. Their simulation results suggest that when meridional winds are changed from 10–40 m/s, growth of the irregularities became half, and hence showed that meridional wind is the key factor for the equinoctial asymmetry. *Ossakow et al.* [1979] have studied the influence of the altitude of the F peak and background electron density gradient length (L) on the generation of spread F irregularities through
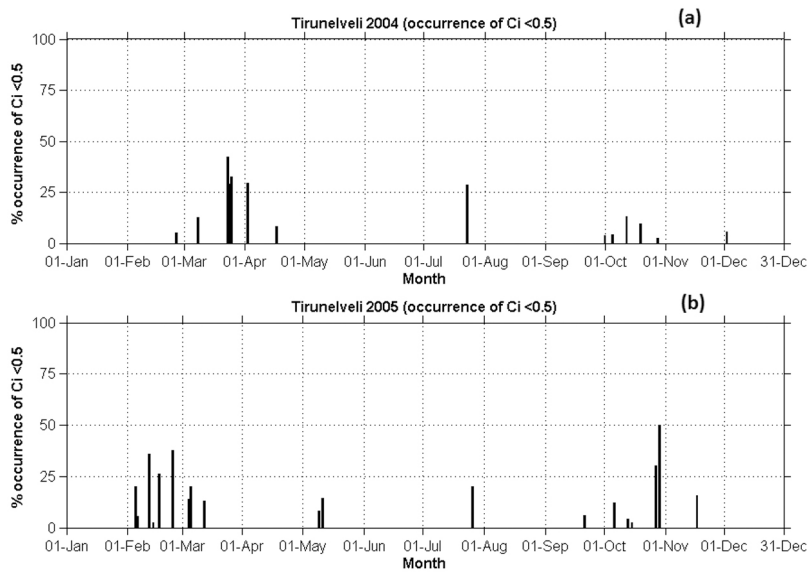
Figure 8. The occurrence percentage of maximum cross-correlation (C_I) < 0.5 in the early phase of the plasma bubble (19:00–22:00 IST) during (a) 2004 and (b) 2005.

nonlinear simulations using different combinations of these two parameters. They found that F peak observed at higher altitude and small background electron density scale length (sharp density gradients) causes higher growth rate of the instability. Recently, *Kil et al.* [2004] have investigated the morphology of the F region plasma density using OI 135.6 nm nightglow images from TIMED/GUVI satellite observations and suggested that enhanced F region electron density is also responsible for the strong ESF activity at most of the longitudes, whereas low plasma density is responsible for suppression of ESF activity. This is supported by our observation that higher F region electron density in vernal equinox period than in autumn equinox period leads to the difference in the growth of the ESF irregularities.

[16] In order to understand the mechanism for the equinoctial asymmetry presented here, we have looked into maximum cross-correlation (C_I) of VHF spaced receiver scintillation records obtained at Tirunelveli (8.7°N, 77.8°E, Dip: 0.4°N) during the years 2004 and 2005, as C_I is used to study the electric field fluctuations in the plasma bubble in the early phase of ESF development [*Bhattacharyya et al.*, 2001]. It is computed at every 3 min intervals by taking the cross-correlation between the two spaced receiver signals, which are separated by a distance of 540 m. A large variation of the drift velocity derived from spaced receiver scintillation observations arises due to electric field perturbations associated with the R-T instability, which cause the plasma bubbles to rise to higher altitudes in the initial phase of the EPB development [*Bhattacharyya et al.*, 2001]. C_I is often found to be <0.5 in the initial phase of EPB development due to presence of perturbation electric fields associated with the R-T instability but remains close to 1 in the later phase under magnetically quiet periods. Using this technique, *Kakad et al.* [2007] have studied the fresh generation of irregularities around midnight hours and suppression of scintillations during pre-midnight hours during magnetically active periods. From *Tiwari et al.* [2006], one can notice that smaller the C_I, higher the maximum height reached by the irregularity layer. *Sripathi et al.* [2008] have studied the latitudinal extent of L-band scintillations during different ESF events. They suggested that when C_I is $\ll 1$, irregularities rise to higher altitudes but when C_I is close to 1, irregularities are confined to lower altitudes. Their study also showed that latitudinal extent of L-band scintillations increases when irregularities rise to higher altitudes, but L-band scintillations are limited to low latitudes when irregularities are confined to bottomside only. Further, they showed that the height of the F layer increases when irregularities rise to higher altitudes whereas height of the F layer do not increase very much when irregularities are confined to bottomside. Hence, we used this concept to say something about height of the irregularity layer in absence of ionosonde data for 2004 and 2005. To study the variation in the occurrence of C_I during different seasons, we have computed the % occurrence of $C_I <= 0.5$ during 19:00–22:00 IST for the years 2004 and 2005. Figures 8a–8b show the percentage occurrence of C_I for the years 2004 and 2005. The figure suggests that the occurrence of C_I is more during vernal equinox than during autumn equinox, indicating that height of the irregularity layer may be higher during vernal equinox than during autumn equinox period. This explains the greater latitudinal extent of L-band scintillations before 22:00 IST during vernal equinox as compared to the autumn equinox. Since we don't have ionosonde observations for the year 2004–2005, we use typical diurnal variation of F layer height over Trivandrum, an equatorial station, during vernal and autumn seasons in the year 2002, when the equinoctial asymmetry in the occurrence of scintillations is seen, as shown in Figures 9a–9b. One can understand from the figure that there is a difference in F layer height during these two equinoxes at ~20:00 IST that is quite similar to that of C_I. It is well known that growth of the ESF irregularities is more when F layer height is higher due to less collision of ions with neutrals. Peak electron density obtained over equatorial and low latitude region also suggests that asymmetric electron density distribution during these two equinox periods in the GUVI observations where electron density in the vernal
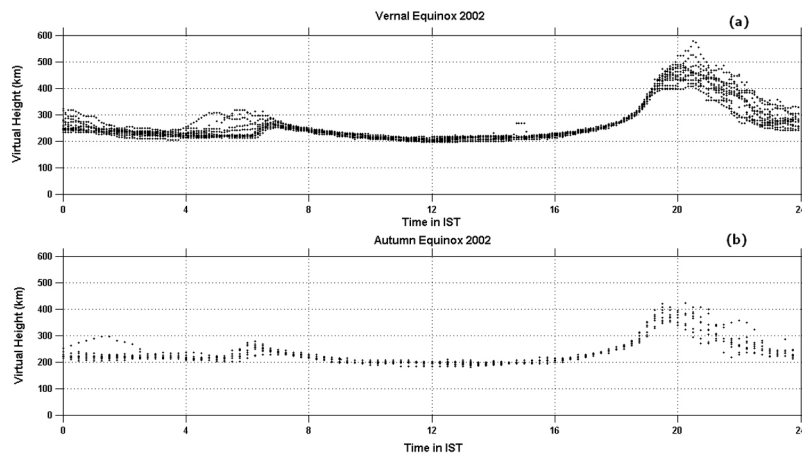
Figure 9. (a–b) The diurnal variation of virtual height of the F layer over Trivandrum, an equatorial station during the year 2002.

equinox period is higher than that of autumn period. Interestingly, MU radar observations also suggested that there exists an asymmetric electron density distribution during these two seasons, hence supporting our observations [*Balan et al.*, 1997]. In order to explain strong L-band scintillations over EIA region, it is suggested that enhanced background electron density accumulated due to fountain effect may provide sharper density gradients leading to stronger and greater scintillation occurrence [e.g., *Bhattacharyya et al.*, 2003]. *Maruyama et al.* [2009] have shown that asymmetric meridional winds during vernal equinox and autumn equinox periods over Indonesia may provide asymmetric growth of the irregularity and leading to the equinoctial asymmetry. In our observations we have seen (1) enhanced background electron density during vernal equinox compared to that of autumn period and (2) symmetry (asymmetry) of northern/southern crests with respect to geomagnetic latitude, during vernal (autumn) equinox, suggesting that transequatorial winds might be different during these two seasons, hence leading to the asymmetry in the occurrence of scintillations. *Jyoti et al.* [2004] have studied the effect of height of F layer and meridional neutral winds on the growth of the ESF irregularities using ionosonde observations over Trivandrum, an equatorial station and SHAR, an off-equatorial location. While this paper did not distinguish between the equinoxes, it showed that when F layer height is above certain threshold, ESF activity is seen irrespective of the direction of meridional neutral winds. However, the direction of meridional winds plays a vital role in excitation of ESF irregularities when the F layer height is below a threshold level. These observations suggest that the F layer height could be below this threshold level during the years 2004–2005, hence the scintillation activity is enhanced or suppressed depending upon the direction and magnitude of the meridional winds. Recently, asymmetry in the background electron density during equinoxes has been studied in detail by *Liu et al.* [2010] and *Ren et al.* [2011] using COSMIC density profiles and ROCSAT-1 drift observations, respectively. They found that plasma densities as well as vertical drifts are more pronounced in vernal equinox than in autumn equinox period over low latitudes. While *Liu et al.* [2010] have suggested that equinoctial asymmetry could be due to manifestation of the annual variation of plasma densities and meridional winds, *Ren et al.* [2011] have suggested that asymmetry in the plasma density could be due to daytime vertical drift. In this paper some of the possible sources for the equinoctial asymmetry in the occurrence of scintillations have been investigated and the results suggest that meridional winds play an important role in the asymmetry. Role of asymmetric E region conductivities at the feet of the field line connecting F region, asymmetric distribution of gravity waves which seed the ESF activity, and asymmetric tidal wind amplitudes that produce asymmetry in the PRE may also be playing vital roles in producing equinoctial asymmetry of the ESF, which will be examined in the future studies.

5. Summary and Conclusions

[17] Amplitude scintillations on the GPS L1 signal recorded at several stations over India and amplitude scintillations on a VHF signal recorded using spaced receivers at an equatorial station are used to investigate the development of ESF irregularities during low solar activity period. The latitudinal and temporal variation of L-band scintillations is found to be quite similar to that of latitudinal and temporal variation of occurrence characteristics of ROTI. Latitudinal and temporal evolution of L-band scintillations show that while weak scintillations occur over equatorial region, stronger scintillations are seen over EIA region, but preferentially during the vernal equinox because the irregularities reach a greater height during the vernal equinox as compared to autumnal equinox so that they may go to higher latitudes, extending up to the EIA region. Our study also indicates that the latitudinal variation of percentage of occurrence of ROTI varies similar to that of L-band scintillations. In addition, the observations also show asymmetry in the occurrence of scintillations in the equinoctial months on both the L-band and VHF-band signals. The results from our analysis using maximum cross-correlation (C_I) derived from spaced receiver VHF scintillation observations suggests that height of the irregularity layer may be different for vernal and autumn equinox periods. TIMED/GUVI satellite measured peak F2 layer density obtained over equatorial region suggest that background electron density may be playing a vital role in providing the equinoctial asymmetry in the occurrence of ESF irregularities.

References

Aarons, J. (1993), The longitudinal morphology of equatorial F-layer irregularities relevant to their occurrence, *Space Sci. Rev.*, *63*, 209–243, doi:10.1007/BF00750769.

Abdu, M. A. (2001), Outstanding problems in the equatorial ionosphere-thermosphere electrodynamics relevant to spread F, *J. Atmos. Sol. Terr. Phys.*, *63*, 869–884, doi:10.1016/S1364-6826(00)00201-7.

Abdu, M. A., J. Bittencourt, and I. Batista (1981), Magnetic declination control of the equatorial F region dynamo electric field development and spread F, *J. Geophys. Res.*, *86*(A13), 11,443–11,446, doi:10.1029/JA086iA13p11443.

Balan, N., Y. Otsuka, and S. Fukao (1997), New aspects in the annual variation of the ionosphere observed by the MU Radar, *Geophys. Res. Lett.*, *24*(18), 2287–2290, doi:10.1029/97GL02184.

Basu, S., and M. C. Kelley (1977), Review of equatorial scintillations phenomena in light of recent developments in the theory and measurement of equatorial irregularities, *J. Atmos. Terr. Phys.*, *39*, 1229–1242, doi:10.1016/0021-9169(77)90032-0.

Basu, S., S. Basu, J. Aarons, J. P. McClure, and M. D. Cousins (1978), On the coexistsence of kilometer- and meter-scale irregularities in the nighttime equatorial F region, *J. Geophys. Res.*, *83*(A9), 4219–4226, doi:10.1029/JA083iA09p04219.

Bhattacharyya, A., K. C. Yeh, and S. J. Franke (1992), Deducing turbulence parameters from transionospheric scintillation measurements, *Space Sci. Rev.*, *61*, 335–386, doi:10.1007/BF00222311.

Bhattacharyya, A., T. L. Beach, S. Basu, and P. M. Kintner (2000), Nighttime equatorial ionosphere: GPS scintillations and differential carrier phase fluctuations, *Radio Sci.*, *35*(1), 209–224, doi:10.1029/1999RS002213.

Bhattacharyya, A., S. Basu, K. M. Groves, C. E. Valladares, and R. Sheehan (2001), Dynamics of equatorial F region irregularities from spaced receiver scintillation observations, *Geophys. Res. Lett.*, *28*(1), 119–122, doi:10.1029/2000GL012288.

Bhattacharyya, A., K. M. Groves, S. Basu, H. Kuunzler, C. E. Valladares, and R. Sheehan (2003), L-band scintillation activity and space-time structure of low-latitude UHF scintillations, *Radio Sci.*, *38*(1), 1004, doi:10.1029/2002RS002711.

Briggs, B. H. (1984), The analysis of spaced sensor records by correlation techniques, in *Middle Atmosphere Program*, *Handbook for MAP*, vol. 13, edited by R. A. Vincent, pp. 166–186, NASA, Washington, D. C.

Burke, W. J., L. C. Gentile, C. Y. Huang, C. E. Valladares, and S. Y. Su (2004), Longitudinal variability of equatorial plasma bubbles observed by DMSP and ROCSAT-1, *J. Geophys. Res.*, *109*, A12301, doi:10.1029/2004JA010583.

Chandra, H., and R. G. Rastogi (1972), Equatorial spread-F over a solar cycle, *Ann. Geophys.*, *28*(4), 709–716.

Dasgupta, A., D. N. Anderson, and J. A. Klobuchar (1983), Equatorial F region ionization differences between March and September, 1979, *Adv. Space Res.*, *10*, 199–202.

DeMajistre, R., L. J. Paxton, D. Morrison, J.-H. Yee, L. P. Goncharenko, and A. B. Christensen (2004), Retrievals of nighttime electron density from Thermosphere Ionosphere Mesosphere Energetics and Dynamics (TIMED) mission Global Ultraviolet Imager (GUVI) measurements, *J. Geophys. Res.*, *109*, A05305, doi:10.1029/2003JA010296.

Devasia, C. V., N. Jyoti, K. S. V. Subbarao, K. S. Viswanathan, D. Tiwari, and R. Sridharan (2002), On the plausible linkage of thermospheric meridional winds with the equatorial spread F, *J. Atmos. Sol. Terr. Phys.*, *64*, 1–12, doi:10.1016/S1364-6826(01)00089-X.

Fejer, B. G., and M. C. Kelley (1980), Ionospheric irregularities, *Rev. Geophys.*, *18*(2), 401–454, doi:10.1029/RG018i002p00401.

Huang, C. Y., W. J. Burke, J. S. Machuzak, L. C. Gentile, and P. J. Sultan (2002), Equatorial plasma bubbles observed by DMSP satellites during a full solar cycle: Toward a global climatology, *J. Geophys. Res.*, *107*(A12), 1434, doi:10.1029/2002JA009452.

Jyoti, N., C. V. Devasia, R. Sridharan, and D. Tiwari (2004), Threshold height (h′F)c for the meridional wind to play a deterministic role in the

bottom side equatorial spread F and its dependence on solar activity, *Geophys. Res. Lett.*, *31*, L12809, doi:10.1029/2004GL019455.

Kakad, B., K. Jeeva, K. U. Nair, and A. Bhattacharyya (2007), Magnetic activity linked generation of nighttime equatorial spread F irregularities, *J. Geophys. Res.*, *112*, A07311, doi:10.1029/2006JA012021.

Kelley, M. C. (2009), *Earth's Ionosphere: Plasma Physics and Electrodynamics*, 2nd ed., Academic, San Diego, Calif.

Kelley, M. C., D. Hysell, and S. Musman (1996), Simultaneous global positioning system and radar observations of equatorial spread F at Kwajalein, *J. Geophys. Res.*, *101*(A2), 2333–2341, doi:10.1029/95JA02025.

Kil, H., R. DeMajistre, and L. J. Paxton (2004), F region plasma distribution seen from TIMED/GUVI and its relation to the equatorial spread F activity, *Geophys. Res. Lett.*, *31*, L05810, doi:10.1029/2003GL018703.

Krishna Moorthy, K. K., C. Raghava Reddi, and B. V. Krishna Murthy (1979), Night-time ionospheric scintillations at the magnetic equator, *J. Atmos. Sol. Terr. Phys.*, *41*, 123–134, doi:10.1016/0021-9169(79)90004-7.

Kumar, K. K., T. M. Antonita, G. Ramkumar, V. Deepa, S. Gurubaran, and R. Rajaram (2007), On the tropospheric origin of Mesosphere Lower Thermosphere region intraseasonal wind variability, *J. Geophys. Res.*, *112*, D07109, doi:10.1029/2006JD007962.

Lee, C.-C., J.-Y. Liu, B. W. Reinisch, W.-S. Chen, and F.-D. Chu (2005), The effects of the pre-reversal drift, the EIA asymmetry, and magnetic activity on the equatorial spread F during solar maximum, *Ann. Geophys.*, *23*, 745–751, doi:10.5194/angeo-23-745-2005.

Liu, L., M. He, X. Yue, B. Ning, and W. Wan (2010), Ionosphere around equinoxes during low solar activity, *J. Geophys. Res.*, *115*, A09307, doi:10.1029/2010JA015318.

Manju, G., C. V. Devasia, and R. Sridharan (2007), On the seasonal variations of the threshold height for the occurrence of equatorial spread F during solar minimum and maximum years, *Ann. Geophys.*, *25*, 855–861, doi:10.5194/angeo-25-855-2007.

Mannucci, A. J., B. A. Iijima, U. J. Lindqwister, X. Pi, L. Sparks, and B. D. Wilson (1999), *GPS and Ionosphere: URSI reviews of Radio Science*, Jet Propul. Lab., Pasadena, Calif.

Maruyama, T., and N. Matuura (1984), Longitudinal variability of annual changes in activity of equatorial spread F and plasma bubbles, *J. Geophys. Res.*, *89*(A12), 10,903–10,912, doi:10.1029/JA089iA12p10903.

Maruyama, T., S. Saito, M. Kawamura, K. Nozaki, J. Krall, and J. D. Huba (2009), Equinoctial asymmetry of a low-latitude ionosphere-thermosphere system and equatorial irregularities: Evidence for meridional wind control, *Ann. Geophys.*, *27*, 2027–2034, doi:10.5194/angeo-27-2027-2009.

Muella, et al. (2008), GPS L-band scintillations and ionospheric irregularity zonal drifts inferred at equatorial and low-latitude regions, *J. Atmos. Terr. Phys.*, *70*, 1261–1272, doi:10.1016/j.jastp.2008.03.013.

Musman, S., J.-M. Jahn, J. LaBelle, and W. E. Swartz (1997), Imaging spread-F structures using GPS observations at Alcântara, Brazil, *Geophys. Res. Lett.*, *24*(13), 1703–1706, doi:10.1029/97GL00834.

Nishioka, M., A. Saito, and T. Tsugawa (2008), Occurrence characteristics of plasma bubble derived from global ground-based GPS receiver networks, *J. Geophys. Res.*, *113*, A05301, doi:10.1029/2007JA012605.

Ossakow, S., S. Zalesak, B. McDonald, and P. Chaturvedi (1979), Nonlinear equatorial spread F: Dependence on altitude of the F peak and bottomside background electron density gradient scale length, *J. Geophys. Res.*, *84*(A1), 17–29, doi:10.1029/JA084iA01p00017.

Otsuka, Y., K. Shiokawa, and T. Ogawa (2006), Equatorial ionospheric scintillations and zonal irregularity drifts observed with closely spaced GPS receivers in Indonesia, *J. Meteorol. Soc. Jpn.*, *84A*, 343–351, doi:10.2151/jmsj.84A.343.

Patra, A. K., D. Tiwari, S. Sripathi, P. B. Rao, R. Sridharan, C. V. Devasia, K. S. Viswanathan, K. S. V. Subbarao, R. Sekar, and A. E. Kherani (2005), Simultaneous radar observations of meter-scale F region irregularities at and off the magnetic equator over India, *J. Geophys. Res.*, *110*, A02307, doi:10.1029/2004JA010565.

Patra, A. K., D. V. Phanikumar, and T. K. Pant (2009), Gadanki radar observations of F region field-aligned irregularities during June solstice of solar minimum: First results and preliminary analysis, *J. Geophys. Res.*, *114*, A12305, doi:10.1029/2009JA014437.

Pi, X., A. J. Mannucci, U. J. Lindqwister, and C. M. Ho (1997), Monitoring of global ionospheric irregularities using the worldwide GPS network, *Geophys. Res. Lett.*, *24*(18), 2283–2286, doi:10.1029/97GL02273.

Rama Rao, P. V. S., S. Gopi Krishna, K. Niranjan, and D. S. V. V. D. Prasad (2006a), Study of spatial and temporal characteristics of L-band scintillations over the Indian low-latitude region and their possible effects on GPS navigation, *Ann. Geophys.*, *24*, 1567–1580, doi:10.5194/angeo-24-1567-2006.

Rama Rao, P. V. S., S. Gopi Krishna, K. Niranjan, and D. S. V. V. D. Prasad (2006b), Temporal and spatial variations in TEC using simultaneous

measurements from the Indian GPS network of receivers during the low solar activity period of 2004–2005, *Ann. Geophys.*, *24*, 3279–3292, doi:10.5194/angeo-24-3279-2006.

Rama Rao, P. V. S., S. Tulasi Ram, S. Gopi Krishna, K. Niranjan, and D. S. V. V. D. Prasad (2006c), Morphological and spectral characteristics of L-band and VHF scintillations and their impact on trans-ionospheric communications, *Earth Planets Space*, *58*, 895–904.

Rastogi, R. G. (1980), Seasonal and solar cycle variations of equatorial spread F in the American sector, *J. Atmos. Terr. Phys.*, *42*, 593–597, doi:10.1016/0021-9169(80)90093-8.

Rastogi, R. G., P. V. Koparkar, and B. M. Pathan (1990), Nighttime radio wave scintillation at equatorial stations in Indian and American zones, *J. Geomagn. Geoelectr.*, *42*, 1–10, doi:10.5636/jgg.42.1.

Ray, S., and A. Dasgupta (2007), Geostationary L-band signal scintillation observations near the crest of equatorial anomaly in the Indian zone, *J. Atmos. Terr. Phys.*, *69*, 500–514, doi:10.1016/j.jastp.2006.09.007.

Ren, Z., W. Wan, L. Liu, Y. Chen, and H. Le (2011), Equinoctial asymmetry of ionospheric vertical plasma drifts and its effect on *F* region plasma density, *J. Geophys. Res.*, *116*, A02308, doi:10.1029/2010JA016081.

Sastri, J. H., K. Sasidharan, V. Subramanyam, and M. Srirama Rao (1979), Seasonal & sunspot-cycle effects in the occurrence of equatorial spread-F configurations, *Indian J. Radio Space Phys.*, *8*, 135–138.

Sripathi, S., S. Bose, A. K. Patra, T. K. Pant, B. Kakad, and A. Bhattacharyya (2008), Simultaneous observations of ESF irregularities over Indian region using radar and GPS, *Ann. Geophys.*, *26*, 3197–3213, doi:10.5194/angeo-26-3197-2008.

Sultan, P. J. (1996), Linear theory and modeling of the Rayleigh-Taylor instability leading to the occurrence of equatorial spread F, *J. Geophys. Res.*, *101*(A12), 26,875–26,891, doi:10.1029/96JA00682.

Tiwari, D., B. Engavale, A. Bhattacharyya, C. V. Devasia, T. K. Pant, and R. Sridharan (2006), Simultaneous radar and spaced receiver VHF scintillation observations of ESF irregularities, *Ann. Geophys.*, *24*, 1419–1427, doi:10.5194/angeo-24-1419-2006.

Tsunoda, R. (1985), Control of the seasonal and longitudinal occurrence of equatorial scintillations by the longitudinal gradient in integrated E region Pedersen conductivity, *J. Geophys. Res.*, *90*(A1), 447–456, doi:10.1029/JA090iA01p00447.

Valladares, C. E., J. Villalobos, R. Sheehan, and M. P. Hagan (2004), Latitudinal extension of low-latitude scintillations measured with a network of GPS receivers, *Ann. Geophys.*, *22*, 3155–3175, doi:10.5194/angeo-22-3155-2004.

Van Dierendonck, A. J., P. Fenton, and J. Klobuchar (1996), Commercial ionospheric scintillation monitoring receiver development and test results, in *Proceedings of the 52nd Annual Meeting of the Institute of Navigation, Cambridge, MA*, pp. 573–582, Inst. of Navig., Manassas, Va.

Yeh, K. C., and C. H. Liu (1982), Radio wave scintillations in the ionosphere, *Proc. IEEE*, *70*(4), 325–378.

A. Bhattacharyya, B. Kakad, and S. Sripathi, Indian Institute of Geomagnetism, Mumbai Headquarters (Panvel campus), Plot 5, Sector 18, Near Kalamboli Highway, New Panvel (W), Navi Mumbai 410218, India. (sripathi@iigs.iigm.res.in)